Front. Environ. Sci. Eng. 2022, 16(2): 19
https://doi.org/10.1007/s11783-021-1453-z

RESEARCH ARTICLE

Biotoxicity evaluation of zinc oxide nanoparticles on bacterial performance of activated sludge at COD, nitrogen, and phosphorus reduction

Hasti Daraei (✉)[1,2], Kimia Toolabian[3], Ian Thompson[4], Guanglei Qiu[5]

1 Environmental Health Engineering Research Center, Kerman University of Medical Sciences, Kerman, Iran
2 Department of Environmental Health Engineering, Faculty of Public Health, Kerman University of Medical Sciences, Kerman, Iran
3 Faculty of Agriculture and natural resources, Lorestan University, Khorramabad, Iran
4 Department of Engineering Science, University of Oxford, Parks Road, Oxford OX1 3PJ, UK
5 School of Environment and Energy, South China University of Technology, Guangzhou 510006, China

HIGHLIGHTS

- ZnO-NP disrupted metabolic/catabolic balance of bacteria by affecting DHA activity.
- ZnO-NPs toxicity was related to Zn^{2+} ion, interaction with cell and ROS generation.
- Exposure to ZnO-NPs resulted in changed bacterial community structure at sludge.
- The change in the EPS content was observed during exposure to ZnO-NPs.

GRAPHIC ABSTRACT

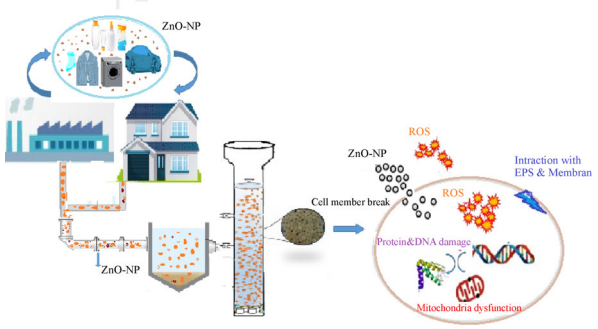

ARTICLE INFO

Article history:
Received 26 October 2020
Revised 3 April 2021
Accepted 18 April 2021
Available online 25 May 2021

Keywords:
Granular sludge
Biotoxicity
Reactive oxygen species
Extracellular polymeric substances

ABSTRACT

The unique properties and growing usage of zinc oxide nanoparticles increase their release in municipal wastewater treatment plants. Therefore, these nanoparticles, by interacting with microorganisms, can fail the suitable functioning of biological systems in treatment plants. For this reason, research into the toxicity of ZnO is urgent. In the present study, the toxicity mechanism of ZnO-NPs towards microbial communities central to granular activated sludge (GAS) performance was assessed over 120-day exposure. The results demonstrate that the biotoxicity of ZnO-NPs is dependent upon its dosage, exposure time, and the extent of reactive oxygen species (ROS) production. Furthermore, GAS performance and the extracellular polymeric substances (EPS) content were significantly reduced at 50 mg/L ZnO-NPs. This exposure led to decreases in the activity of ammonia monooxygenase (25.2%) and nitrate reductase (11.9%) activity. The Field emission scanning electron microscopy images confirmed that ZnO-NPs were able to disrupt the cell membrane integrity and lead to cell/bacterial death via intracellular ROS generation which was confirmed by the Confocal Laser Scanning Microscopy analysis. After exposure to the NPs, the bacterial community composition shifted to one dominated by Gram-positive bacteria. The results of this study could help to develop environmental standards and regulations for NPs applications and emissions.

1 Introduction

The unique properties of NPs have led to their widespread use in industrial, agricultural, medical and health products (Mu et al., 2012). Their high reactivity can cause their harmful interactions with biological systems, which can act as a toxin to the environment (Kaegi et al., 2011) whilst the small size also enables them to penetrate deeper into biological systems not accessible to larger particles (Kim et al., 2010). ZnO-NPs are one of the most widely used NPs because of their high thermal conductivity and stability, their UV absorption and antibacterial properties;

✉ Corresponding author
E-mail: h.daraei@kmu.ac.ir

used in many products such as sunscreen, plastic containers, food, cosmetics (Jiang et al., 2009).

A key concern is that a likely site for released ZnO-NP to accumulate is wastewater treatment plants (WWTPs). Activated sludge (AS) processes such as granular activated sludge (GAS) rely on the ability of microorganisms to convert organic matter into various gases, cellular materials and clean water. GAS is a dense mass of millions of diverse species including bacteria, proteases, fungi and rotifers and has several benefits compare to conventional AS processes such as a compact structure, better stability, fast settling, high biomass and high density of extracellular polymeric substances (EPSs) that protects bacteria from external stress (Gottschalk et al., 2009). Due to the diffusion gradient of nutrients and oxygen, three distinct bacterial regions are formed in aerobic granules (Yang et al., 2013). Aerobic heterotrophic microorganisms and some autotrophs, such as nitrifiers, are located in the outer layers of GAS, whereas facultative and anaerobic bacteria such as denitrifiers and polyphosphate-accumulating organisms (PAO) are present on the inner parts of the GAS. Then, simultaneous removal of organic matter, nitrogen and phosphorus in this process is possible (Arnaout, 2012). Therefore, it is important that the physical-chemical properties of the microorganisms in the GAS remain fit for purpose and stable to ensure the normal operation of a treatment plant (Kim et al., 2010).

The increasing widespread use of NPs can lead to their continuous discharge and entry into WWTP, and thus their potential impact on the functioning of microbial communities in GAS has raised widespread concerns (Yang et al., 2013).

Studied demonstrate that large amounts of NPs can absorb on the surface structure of GAS after addition. Therefore, the interaction of the GAS with the potentially toxic NPs may adversely affect the performance of the biomass bacteria and thus the effective functioning of the WWTP (Corry, 2008, Daraei et al., 2010). Gonzalez-Estrella et al. (2013) investigated the toxicity of ZnO-NPs on methanogenic and acidogenic activity in anaerobic sludge and showed that NPs inhibited the methanogenesis process by up to 50%. Zheng et al. (2011) demonstrated that the inhibition of nitrogen and phosphorus removal was due to the release of zinc ions and increased ROS, which had an inhibitory effect on the enzymatic activity of the bacteria.

The focus of this study was to investigate the response of AS microbial communities to exposure ZnO-NPs. This was evaluated on the basis of reactor performance in terms of the removal of chemical oxygen demand (COD), nitrogen and phosphorus, and enzymatic activities, and dynamics in the bacterial community. Whereas, EPSs as a jelly-like matrix protect the bacteria in activated sludge, the change in the composition of EPS was surveyed as a main stress-response mechanism of bacteria to ZnO-NPs. Also, Confocal Laser Scanning Microscopy (CLSM) was used to visualize the distribution of living/dead cells in GAS–nanoparticle interactions. Whereas, the impact of NPs on real microbial communities in the environment can provide important insight as to the interaction of NPs with the microorganisms and alert us to the potential risks, so for this aim, a rapid, valid and accurate metagenomic analysis method Used to identify the abundance of bacteria in the granular sludge.

2 Materials and methods

2.1 Preparation of ZnO-NPs

ZnO-NPs with a mean diameter of less than 50 nm (purity 99.9%) were purchased from Sigma Co., USA. The ZnO-NPs stock suspension (1000 mg/L) was prepared daily. To disperse the aggregated NPs, the stock solution was sonicated for 1 h (30 °C, 250 W, 40 kHz) and then concentrations of 1, 10 and 50 mg/L were prepared from the stock suspension. The particle size distribution was determined using the DLS and the mean diameter of the nanoparticles in suspension was 45 nm (Yazdanbakhsh et al., 2019).

2.2 The granular SBR set up and operation

Experiments were conducted in 4 pilot-scale sequencing batch reactors (SBR) for the ZnO-NPs exposure tests (0–50 mg/L). The reactors were designed with a working volume of 1 L and a height/diameter (H/D) of 8/1. All reactors had six 4-hour cycles per day with sequential phases of feeding (2 min), reaction (220 min), settling (1 min), discharge (1 min) and idle (17 min). In order to aerate and mix the liquid, air diffusers were installed at the bottom of the reactors with a flow rate of approximately 3L/min. To create aerobic and anoxic conditions, dissolved oxygen was kept in the range of 2.0–2.5 mg/L and 0.15–0.5 mg/l, respectively (Yazdanbakhsh et al., 2019).

All of the above steps in the reactors were performed automatically using a programmable logic controller (PLC). AS collected from the aeration basin of a municipal WWTPs (MLSS = 3900 mg/L, SVI = 185 mL/g) was used as inoculum. The reactors were fed with synthetic wastewater that was prepared of sodium acetate and glucose (COD = 1500 mg/L), NH^{+}_{4} 40, PO_4^{3-} 10, and trace elements including $FeCl_3.6H_2O$, H_3BO_3, $CuSO_4.5H_2O$, KI, $MnCl_2.4H_2O$, $NaMoO_4.2H_2O$, $CoCl_2.6H_2O$ (Yazdanbakhsh et al., 2019). GAS was formed with a diameter of 2–3 mm after about two months. The granular sludge was operated for 1 month to achieve steady-state in the removal of COD, TN and TP (approximately 94%, 74% and 70%), then the ZnO-NPs exposure experiments were performed at four concentrations (0, 1, 10 and 50 mg/L) to evaluate

their potential toxicity on GAS. The exposure time of GAS to ZnO-NPs was 120 days and during the exposure period (1 to 120 days) chemical and biological tests were performed on GAS and effluent.

2.3 Determination of ROS generation

The intracellular ROS produced was determined using dichlorodihydrofluorescein diacetate reagent (H_2-DCFDA). This reagent exclusively identifies reactive oxygen intermediates by generating fluorescent. For this purpose, the GAS samples (before and after exposure to the ZnO-NPs) were centrifuged at 100 g for 5 min and then washed three times with 0.1 mg/L phosphate buffer (PBS). The granules were stained by suspending in H2-DCFDA solution diluted with phosphate buffer and incubated in the dark at 37°C for 30 min. The granules were centrifuged and washed again with 1× PBS and transferred to a 96-well plate. Finally, the generated signal was read after 4 hours using a microplate reader at Ex/Em = 485/535 nm (Mu and Chen, 2011).

2.4 Extraction and analysis of Extracellular Polymeric Substances (EPS)

The extraction of EPS was based on a heating-physical extraction method. Whereas polysaccharide (PS), humic substances (HS) and proteins (PN) are considered as the main components of EPS in sludge, so total EPSs was reported as the sum of PN, PS and HS. 20 mL of the mixed liquid were withdrawn and placed in a water bath at 60°C for 30 min. Then the samples were centrifuged at 20000 g for 15 min at 4°C. The supernatant was filtered through a 0.22-μm membrane, and finally, its protein (PN), polysaccharide (PS) and humic substance contents were measured and reported as total EPS. PS was determined using phenol/sulfuric acid method and 0-100 mg/L glucose solution as standard. Protein was measured with the brilliant blue method and 0–250 mg/L BSA as standard. The humic substance was determined by the modified Lowry method using humic acid as standard (Deng et al., 2016).

2.5 Distribution of live/dead cells in GAS by Confocal Laser Scanning Microscope

To better understand the effect of ZnO-NPs on the sludge viability, the distribution of live and dead cells was investigated using CLSM (Leica TCS SPE, Germany). SYTO63 and SYTOX Blue (Molecular Probes, Carlsbad, CA, USA) were used to identify live (red) and dead cells (light blue) in the granules, respectively. Briefly, GAS before and after ZnO-NPs exposure (0 and 50 mg/L) were withdrawn from the reactor and were washed with deionized water. Then 20 μM of SYTO63 was added to the granules and shaken for 30 minutes. The samples were then washed twice with 1× PBS to remove excess dye. Subsequently, 2.5 μM of SYTOX Blue was added to the sample and incubated for 5 minutes. Then the stained samples were frozen at –20°C and finally were sectioned into 30 μm portions using a microtome. The sectioned granules were placed on a microscopic slide and their internal structure was observed by CLSM. SYTO 63 was detected with excitation at 633 nm and emission at 700–650 nm. SYTOX Blue was detected with excitation at 405 nm and emission at 460–500 nm (Quan et al., 2015; Mu et al., 2012).

2.6 DNA extraction and purification to analysis of bacterial community dynamics

GAS samples were collected from the SBRs and were immediately kept at-80ºC until DNA extraction. Briefly, GAS samples were centrifuged and their genomic DNA was extracted using Fast DNA ™ kit for soil (MP Biomedicals LLC; Cat. 116540600) following the manufacturer's instructions. DNA integrity and concentration were tested by gel electrophoresis and a Qubit fluorometer, respectively. For the gene library construction, the bacterial 16S rRNA was amplified using universal bacterial primer pair (515 FB: 5': GTGYCAGCMGCCGCGGTAA: 3'; 926 RB: 5': CCGYCAATTYMTTTRAGTTT: 3') by PCR. The PCR was run at steps 95°C for 30 s, 35 cycles of denaturing (5 s at 95°C), annealing (34 s at 63°C), and a melting curve analysis from 60°C to 95°C. About 50 μL of purified DNA withdrawn and Illumina HiSeq 2000 platform was used to sequence the microbial population in the sludge samples. The operational taxonomic units (OTUs) for obtained sequences were identified using the Qiime software. Finally, all raw datasets obtained were searched at the NCBI-nr database and BLASTX for reconnaissance of reference bacteria www.ncb.nlm.nih.gov/BLAST) (Daraei et al., 2019).

2.7 Analytical methods and statistical analysis

Reactors' performances such as removal efficiency of COD, TN, TP as well as Zn^{2+} concentration in wastewater were measured according to the standard method (APHA, 2005). Morphological characteristics of GAS before and after ZnO-NPs treatment were observed via FESEM microscope (SU5000, HITACHI). The activities of seven key enzymes including the dehydrogenase (DHA), ammonia monooxygenase (AMO), nitrite oxidoreductase (NOR), nitrite reductase (NIR), nitrate reductase (NR), polyphosphate kinase (PPK), and exopolyphosphatase (PPX) were assessed following the report of Yazdanbakhsh et al. (2019). These enzymes were investigated since they are associated with the removal of COD, N and P, respectively.

3 Results and discussion

3.1 Field emission scanning electron microscopy (FESEM)

The morphology and apparent integrity of the GAS samples before and after exposure to the ZnO-NPs was observed by FESEM (Fig. 1). Microscopy images confirmed the high abundance of filamentous, spherical, and rod bacteria in the granules (Fig. 1(a)). Integration of bacteria and filaments in granules in the absence of NPs is clearly seen and cocci and rods were attached together by a multitude of filaments and polymers secreted from them. The polymers-like substances may have acted as a barrier to protect of the internal bacteria against stressors (Liang et al., 2010). GAS structures after exposure to the ZnO-NPs are shown in Figs. 1(b)–1(d), respectively. Figures 1 (b) and 1(c) showed that exposure to 1 mg/L ZnO-NPs had no serious damage to the GAS structure. A large number of NPs were adsorbed on the surface of filaments and possibly EPS. Figure 1(d) shows significant variations in GAS morphology after exposure to 50 mg ZnO-NP/L. High doses of ZnO-NPs caused morphological variations and dehydration in filamentous bacteria located at the granule surface. On the other hand, damage to the filaments prevents bio-granulation and also leads to penetration of the ZnO-NPs/ Zn^{2+} into the inner parts of the granules. Mu and Chen (2011) reported that that ions released from ZnO-NPs could be adsorbed onto the surface of the granule and EPS, and reduced the toxicity of NPs towards exposed microorganisms. Mu and Chen (2011) found that ZnO-NPs are adsorbed on sludge by three mechanisms including adsorption; sorption on EPS; and absorption, and thus activated sludge can play an important role in preventing or at least reducing the release of NPs into the environment.

3.2 Effects of ZnO-NPs on SBRs performance

The effect of ZnO-NPs on the removal of COD, TN and TP was investigated. The compact structure of granular sludge is composed of a high density of biomass and a diverse community of bacteria. Due to the penetration gradient of different compounds in the granules and the presence of various microbial masses, simultaneous removal of organic matter, nitrogen and phosphorus in a reactor is possible (Mu and Chen, 2011). GASs are composed of three different bacterial regions. The outer layer is aerobic bacteria and the inner parts were anoxic and anaerobic bacteria, which provide microenvironments for the simultaneous nitrification/denitrification process and phosphorus removal (Zheng et al., 2011). In the SBR dosed with 1mg ZnO-NPs/L, the removal of COD, TN and TP were almost constant and remained at 95.7%, 71.6% and 70.4%, respectively (Fig. 2). The values are comparable to these in the control reactor (96.1%, 71.1% and 68.8%) ($p = 0.512$). 10 mg ZnO-NPs /L had a slight inhibitory effect on the removal of COD and TN (88.5% and 64.6%) ($p < 0.001$) and TP removal was largely similar to the control SBRs (65.7%, $p = 0.506$). In contrast, 50 mg NPs/L decreased the removal efficiency of COD, TN and TP to 67.7%, 52.2% and 47.2%, respectively ($p < 0.001$). The performance of GAS depends on heterotrophic and autotrophic microorganisms, which have the ability to resist low doses of toxic compounds and are able to adapt to toxic conditions in the long term (Zheng et al., 2006). Also, zinc ion is an essential trace element for bacterial growth and activity; therefore, these may be a reason for the high removal efficiency in 1 mg ZnO-NPs/L (Mu et al., 2012). Cocci and rods bacteria have a significant impact on the removal of organic and inorganic compounds that are protected by filaments on the granule surface. This could also have been a reason for the better performance of GAS at low NPs concentrations (> 10 mg/L). At high ZnO-NPs dosage, damage to the filaments resulted in the loss of granule integrity and the formation of cavities at GAS surface (FESEM images confirm this subject). These cavities can be a pathway for penetration of the ZnO-NPs/ Zn^{2+} into the inner parts of GAS, and damage the bacteria that were located there. This may explain the reduced reactor performance when amended with 50 mg NPs/L. Biological removal of ammonia is accomplished by a sequential nitrification process, which is carried out by ammonium-oxidizing bacteria (AOB) and nitrite-oxidizing bacteria (NOB). Nitrifiers are located in the inner layers of the granule and are less affected by stressors (Quan et al., 2015). The penetration of NPs/Zn^{2+} at high concentrations into the granule (due to destruction of the GAS surface), resulted in inhibition of nitrifiers and denitrifiers. Therefore, the decrease in TN removal efficiency may be attributed to the inhibition of the activity of nitrifiers and

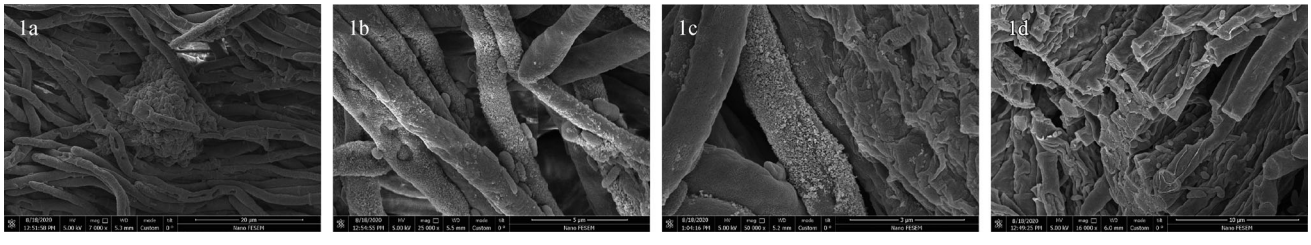

Fig. 1 FESEM images of GAS exposed to (a) 0 mg/L (control), (b) 1mg/L, (c) 10 mg/L and (d) 50 mg/L ZnO-NPs.

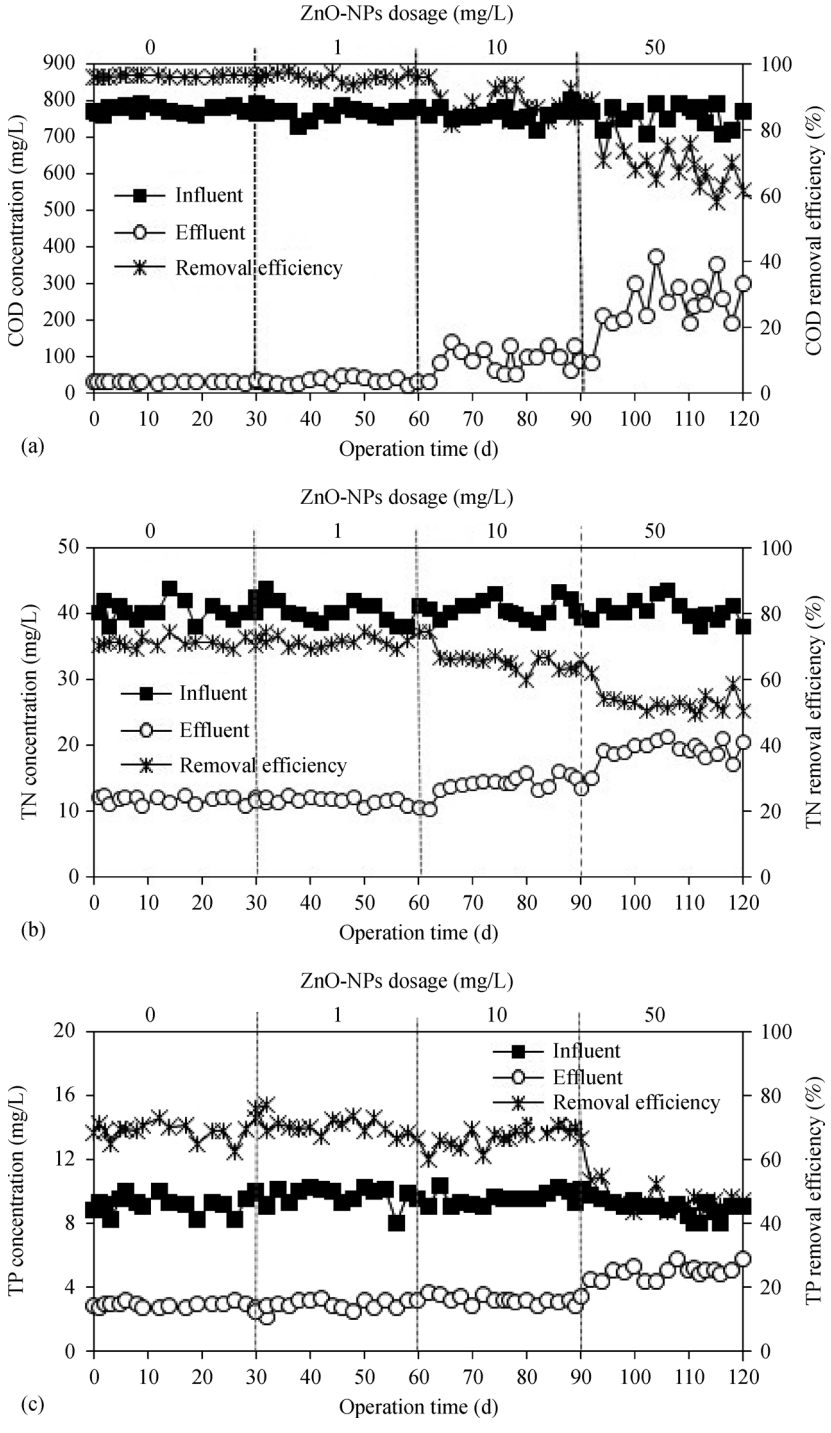

Fig. 2 Performance of GAS at different ZnO-NPs dosages (a) COD, (b) TN, (c) TP comparing influent and effluent.

denitrifiers. However, studies have shown that denitrifiers are less sensitive than nitrifiers and more able to adapt to environmental changes. Yang et al. (2013) reported that nitrifiers are one of the most sensitive bacterial in AS that are strongly affected by stressors such as NPs. Marcilhac et al. (2014) reported that nitrifiers are sensitive bacterial groups present in the sludge, especially NOB, thus the decrease in the growth and abundance of NOB present in the SBR completely inhibits the oxidation of NO^{2-}-N to NO^{3-}-N. Based on these results, the phosphorus removal efficiency was improved when exposed to 1 and 10 mg ZnO-NPs /L. Li et al. (2017) suggested that by adsorption of NPs on the outer sludge layer, the rate of O_2 transfer into the inner sludge layers was reduced and a more suitable environment was provided for the anoxic/anaerobic bacteria. In contrast, 50 mg/L NPs had a remarkable effect

on the TP removal efficiency. The results of this study showed that polyphosphate accumulating organisms (PAO) were sensitive to high doses of ZnO-NPs and were inhibited by exposure to NPs (Zheng et al., 2011).

3.3 Effect of ZnO-NPs on enzymatic activity of GAS

The performance of biological processes in the removal of contaminants is dependent upon their bacterial enzymatic activity. Fig. 3 represents the effect of ZnO-NPs at different dosages on the enzymatic activity of GAS. The Dehydrogenase (DHA) activity was relatively constant at 1–10 mg/L ZnO-NPs ($p > 0.05$), in contrast, declined by 15.53% in 50 mg/L ZnO-NPs compared with the control. DHA is an essential enzyme in the respiratory activity of bacteria and has a significant role in the degradation of organic carbon and carbohydrates. Injection of NPs into the SBR can disrupt the metabolic/catabolic balance of the bacteria by affecting the DHA activity and thus lead to the accumulation of organic matter in the reactor (Kiser et al., 2010). Li et al. (2017) reported that the DHA activity of bacteria is associated with the consumption of oxygen, so changes in SOUR and COD removal efficiency can be attributed to changes in this enzyme activity. Yazdanbakhsh et al. (2019) demonstrated that the DHA can be used as an indicator to determine the viability of bacteria.

In the biological nitrogen removal process, ammonia oxidation to nitrite and subsequently to nitrate is catalyzed by ammonia monooxygenase (AMO) and nitrite oxidoreductase (NOR), respectively. Denitrification is related to biochemical reactions catalyzed by nitrate reductase (NAR) and nitrite reductase (NIR) (Labbe et al., 2003). According to Fig. 2, 1 mg ZnO-NPs/L had no measurable impact on the activity of the nitrifiers' enzymes, even partly increased the NIR and NAR activity. The AMO, NOR, NIR and NAR had slight variations at 10 mg NPs/L as compared to the control rector (5.7%, 2%, 5.4% and 2.53%). In contrast, upon exposure to 50 mg NPs/L, the activities of AMO, NOR, NIR, NR decreased by about 25.2%, 11.9%, 9.9% and 8.03% as compared to the control, respectively. Under 50 mg ZnO-NPs/L, AMO and NOR activities were significantly affected compared to denitrification enzymes, implying that nitrifiers are more sensitive to NPs. Therefore, Therefore, in view of the more pronounced decrease in the AMO and NOR activity in the present study, it may be concluded that nitrification is a critical step in biological nitrogen removal under ZnO-NPs stress (Daraei et al., 2019). Choi et al. (2009) noted that under stress conditions, heterotrophs grow faster than nitrifiers, and are usually less sensitive to external inhibitors and shocks. NAR and NIR activity were less affected by the ZnO-NPs, showing that the heterotrophic denitrifiers grew faster and were less sensitive to the NPs compared to the nitrifiers. Labbe et al. (2003) demonstrated that the activity of denitrification enzymes was related to some metal ions (such as zinc and copper) and low levels of these ions can significantly increase the denitrification rate. Therefore, one of the reasons that 1 mg ZnO NPs/L have no effect on TN removal can be attributed to the positive effect of Zn^{2+} ion on NAR and NIR activity. At 50 mg ZnO-NPs/L, the polyphosphate kinase (PPK), and exopolyphosphatase (PPX) activities reduced by 11.6% and 17.8% by comparison with the control. Whereas the low concentrations of ZnO-NPs (< 10 mg/L) had no detectable significant effect on the PPX and PPK activity. The hydrolysis, synthesis and absorption of polyphosphate were catalyzed by PPX and PPK, respectively (Mu et al., 2012). According to the results, the ZnO-NPs had a greater inhibitory effect on the PPK enzyme, which was related to the removal of phosphorus in aerobic conditions. Zheng et al. (2011) reported that exposure to ZnO-NPs could notably decrease phosphorus removal efficiency by inhibiting PPX and PPK activities. Chen et al. (2012) explained that most NPs could decrease the enzymatic activity of the bacteria by absorbing the essential microelement (which is needed for bacteria) in the wastewater. In general, some enzymes alone are unable to catalyze metabolic activities and require some activators (such as co-factors) to improve their catalytic activity. In fact, these metal ions are one of

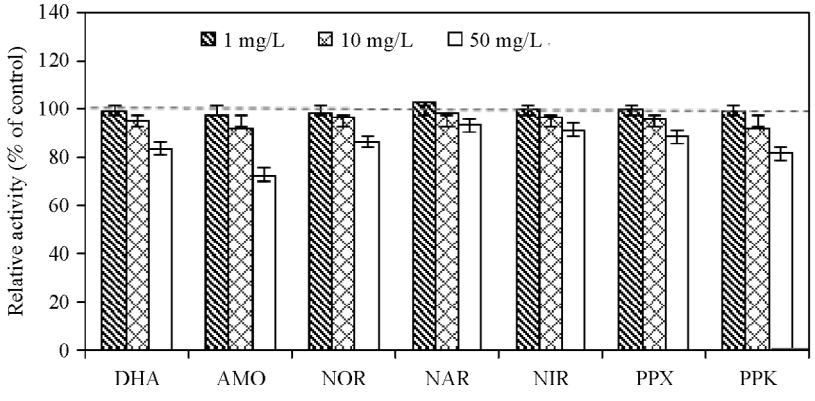

Fig. 3 ZnO-NPs impact on the enzymatic activities; DHA, AMO, NOR, NAR, NIR, PPX, PPK. Error bars display SD of triplicate experiments.

the essential active sites for bonding the substrate to the enzyme molecules (Daraei et al., 2019). This could be a rational reason to justify the improvement of the performance of activated sludge exposed to low ZnO-NPs dosage.

3.4 Extracellular polymeric substances (EPS) content during ZnO-NPs dosing

The change in the EPS content during exposure to NP is shown in Table 1. Exposure to 1 mg/L ZnO-NPs increased the EPS content, and this may indicate the role of EPS as a defense mechanism which secreted by bacteria cells. It is widely accepted that EPS acts like a skeleton and bind microorganisms together to form granular sludge and acts as a barrier to protect the inner microorganisms from external stress and damage. So as a result, bacteria in AS exposed to low dosages of NPs exhibit their defense response by increasing EPS secretion (Ni et al., 2013).

In contrast, proteins, polysaccharides and humic substances content decreased in exposure to 10 and 50 mg/L ZnO-NPs, and this caused a decline in granulation ability. The average concentration of PN, PS and HS were 113.3±0.7, 72.1±1.2 and 10.4±0.2 mg/g MLVSS prior to exposure to 50 mg ZnO-NPs/L. As seen in the FESEM images, large amounts of NPs were adsorbed on the surface structure of GAS after addition. Previous studies have confirmed the adsorption of NPs on the EPS surface and expressed that EPS can absorb NPs onto the GAS surface through various mechanisms such as forming complexes with EPS compounds, van der Waals forces, electrostatic attraction, and hydrophobic interaction (van der Waals forces). The adsorption of ZnO-NPs caused the decline of the EPS secretion. Since the formation and stableness of GAS is highly dependent on EPS, therefore, this decline in its content could have caused the granule deterioration and decreased reactor performance (Ni et al., 2013; Sheng et al., 2010). Previous findings by other researchers have reported that proteins were the main content of the total EPS; however, with exposure to high NPs doses, its concentration decreased significantly (Deng et al., 2016) which is similar to our finding.

3.5 Determination of ROS generation and released Zn^{2+} ion

Previous studies have identified the basic mechanisms for the toxicity of ZnO-NPs as follows: a) release of antimicrobial Zn^{2+} ions; b) direct interaction of ZnO-NPs/ Zn^{2+} with cell well or DNA and disturbance of cell function, c) disruption of cell membrane integrity, and d) ROS generation due to the interaction of NPs with the media (Tan et al., 2015). The released ions content from the ZnO-NPs was analyzed with inductively coupled plasma mass spectrometry (ICP-MS). The results showed that the degree of solubility of zinc was low in the mixed liquor and the injection of 1, 10, and 50 mg ZnO-NPs /L into the reactors resulted in the release of 0.57, 2.27 and 3.96 mg of Zn^{2+} ions. The release of free Zn^{2+} ions depends on the amount of NPs dissolved in the aqueous medium. In the present study, the results showed that the degree of solubility of zinc was low in the mixed liquor. Based on the reactors' performance in COD, TN and TP removal, it can be concluded that Zn^{2+} ion at low concentrations had a positive impact on the bacteria function in SBRs and bacteria use the Zn^{2+} resealed from NPs as a trace element for their enzymatic activity (Tan et al., 20152015). Mu et al. (2012) reported that the presence of negative charge at the EPS surface provides sites for Zn^{2+} binding and chelating, therefore prevents the influence of Zn into the granule and can decrease the toxicity of Zn^{2+}. In contrast, the high NPs dose released more ions, which was higher than the absorption capacity of the EPS, so increasing its toxicity. Siddiqi et al. (2018) explained that the ZnO-NPs toxicity is mainly related to their concentration/ solubility and the exposure time. Mu and Chen (2011) stated that Zn^{2+} was the main reason for the inhibition of bacterial cell growth by damaging the bacterial cell walls, penetrating into the cell, and binding to the cell's biomolecules. To investigate the biotoxicity of ZnO-NPs, ROS test was performed and the result is shown in Fig. 4. According to the results, 1 and 10 mg ZnO-NPs/L had no significant effect on ROS production. Whereas, ROS production in the 50 mg/L NPs increased by 120% ($p < 0.05$), suggesting that ZnO-NP dosage has a major role in its cytotoxic effect. ROS include superoxide (O_2•), hydrogen peroxide (H_2O_2), and hydroxyl radical (OH•) that are produced in the presence of oxygen (Daraei et al., 2019). Previous studies have shown that ROS can be formed in two ways in the system. First, NPs can be directly absorbed onto the cell's oxidative organs and then produce oxidative stress by stimulating redox-active proteins. Second, the released ions from NPs can produce ROS by undergoing chemical reactions in the presence of oxygen and light (Decker and Lohmann-Mattes. 1988). Yamamoto et al. (2004) noted that the presence of ROS, such as H_2O_2, strongly inhibited bacterial activity. Also, studies have shown that ROS produced can damage cell DNA and lead to cell death. Toxicology studies have explained that ROS generated by

Table 1 Effect of ZnO-NPs on the Compositions of EPS at GAS

Components of EPS	Control	1 mg/L	10 mg/L	50 mg/L
Proteins (mg/g MLVSS)	139.115±1.2	152.4±2.2	132.9±1.7	111.3±0.7
Polysaccharides (mg/g MLVSS)	87.255±1.7	91.4±1.13	79.16±2.24	72.1±1.2
Humic substances (mg/g MLVSS)	22.44±1.1	19.8±1.2	17.35±1.17	12.4±0.2

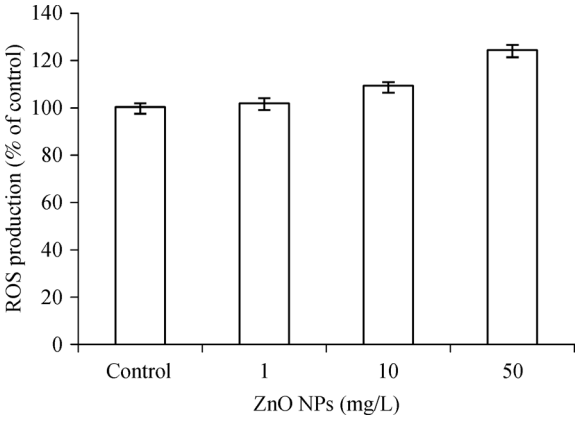

Fig. 4 ROS production of GAS at different ZnO-NPs dosages. Error bars display SD of triplicate experiments.

engineered NPs are able to place cells under oxidative stress and disrupt their normal function by increasing the permeability of the inner membrane (Weinberg et al., 2010). Chen et al. (2012) explained that ROS produced by nanoparticles disrupts cellular antioxidant mechanisms by reducing the activity of vital enzymes such as catalase.

3.6 Distribution of live and dead cells in aerobic granules

Fluorescent staining and CLSM analysis were used to investigate the distribution of living and dead cells in the GAS in the absence and presence of 50 mg ZnO NPs/L (Fig. 5). In the absence of NPs, there were high counts of living cells (red) both on the outer and inner surfaces of the granules, although their distribution on the outer surface was more compact and bolder (Fig. 5-a2). The outer layer of the granule showed a compact, coherent structure with a uniform cell distribution. Fig. 5-a3, displays a layer of dead cells with less abundance located in the inner parts of the granule (blue). The presence of dead cells in the granule may be a reason for the uneven distribution of substrate and DO in the inner part of the GAS, causing some cells to enter the death phase (Yang et al., 2013). In the presence of 50 mg ZnO-NPs /L (Fig.5b), the density of living cells decreased (the reduction in intensity of red color) compared to the control sample and its outer layer was relatively loose and disintegrated. According to Fig. 3b the NPs led to the death of cells in the outer layer and thus created holes in the surface of the granule. These holes could be sites for penetration of NPs or their released ions. As the NPs penetrated into the granule, the viability of cells in the GAS decreased and the abundance of dead cells in the granule increased. The increase in the distribution of dead cells in the presence of ZnO-NPs confirmed the decrease in the enzymatic activity of bacteria as well as the decrease in reactor performance (Labbe et al., 2003).

3.7 Dynamics in bacterial community under ZnO-NPs stress

The diversity and abundance of bacterial populations in GAS before and after exposure to ZnO NPs was

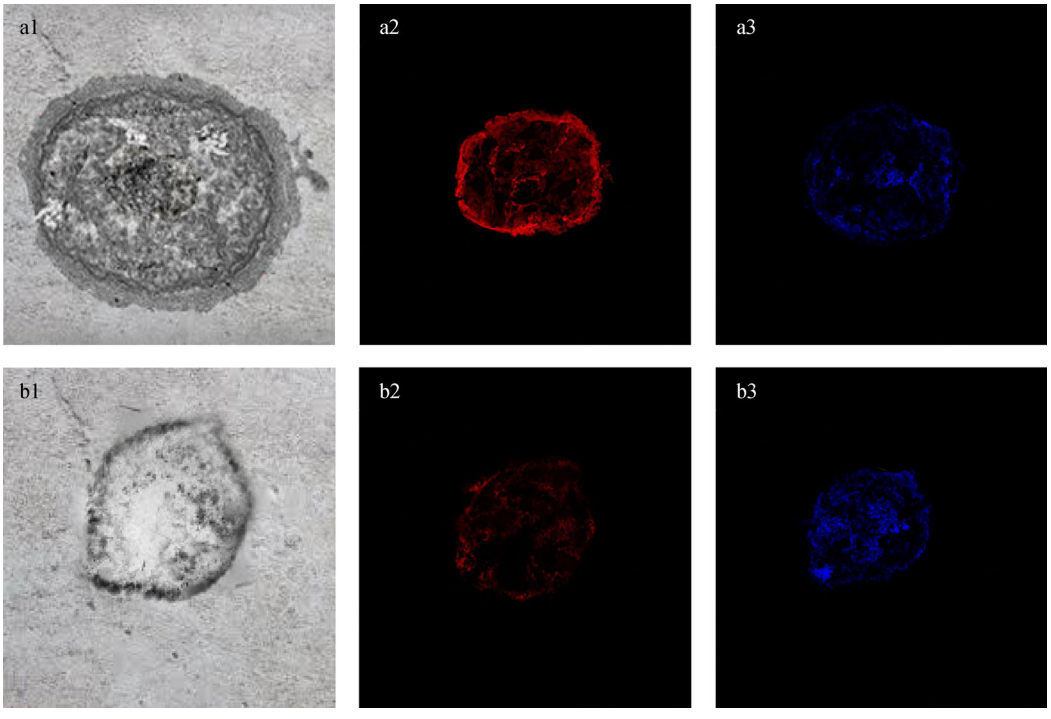

Fig. 5 Distribution profiles of dead and live cells in GAS in the absence (a1-a3) and presence (b1−b3) of 50 mg ZnO-NP/L with SYTO63 (live cell, red), and SYTOX Blue (dead cell, blue).

investigated with the metagenomics method (16S rRNA gene amplicon analysis). Information on bacterial varieties at phyla (Fig. 6) and genus (Fig. 7) levels were provided. The OTU results showed that almost all bacteria were present in the GAS samples (0-50 mg/L) during the experiment and only their abundance changed. The bacterial OTUs showed that *Proteobacteria*, *Firmicutes*, *Bacteroidetes*, and *Actinobacteria* were the predominant bacteria before and after exposure to the ZnO-NPs. Studies have shown that these phyla have an important role in flocculation and biological treatment (Zheng et al., 2011; Sheng et al., 20102012). The other phyla (with abundance of less than 1%) were *Deinococcus–Thermus*, *Armatimonadetes* and *Chlamydiae*. *Archaea* were also identified and the dominant phylum belonged to *Euryarchaeota* species. Li et al. (2013) reported that *Euryarchaeota* is one of the main methanogens. Before NPsexposure, the abundance of *Proteobacteria*, *Firmicutes*, *Bacteroidetes* were 49%, 14.5% and 12%, respectively. In 1 mg NPs/L, the change in bacterial abundance was negligible. In contrast, exposure to 50 mg/L ZnO-NPs resulted in decreased relative abundances of *Proteobacteria*, *Bacteroidetes*, and *Nitrospirae*; on the other hand, *Firmicutes* become increasingly dominated. *Armatimonadetes* were not detected after injection of nanoparticles. Exposure to 10 mg NP/L changed slightly the bacterial community structure reactor. In fact, trace concentrations of metal ions are essential micronutrients for bacteria (Sheng et al., 2010). In general, the results indicated that ZnO-NPs reduced the relative abundances of Gram-negative bacteria (such as *Proteobacteria*) in compared with Gram-positive bacteria (such as *Firmicutes*). Sirelkhatim et al. (2015) described that in Gram-positive bacteria, biomolecules and other intracellular contents are protected by a multilayer membrane matrix as well as a cell wall with a thickness of 10–80 nm. In contrast, Gram-negative bacteria have a thin cell membrane (about 7 nm), and this permits the passage of NPs into the cell which can result in the cell can disruption of cell metabolism and reproduction. *Proteobacteria* play an important role in the simultaneous removal of organics, nitrogen and phosphorus in wastewater (Zheng et al., 2011). Therefore, decrease in the *Proteobacteria* population led to a decrease in biological treatment efficiency. *Nitrospirae* is one of the main nitrite-oxidizing bacteria in the second step of nitrification, which is also able to convert ammonia to nitrite (Yang et al., 2013). The low abundance of this bacterium (7.6%) in the sludge sample indicates that biological removal of ammonia can be done simultaneously by autotrophs and heterotrophic nitrifiers (Kiser et al., 2010). To better understand the change in bacterial community diversity in the absence and presence of ZnO-NPs, a heat map analysis

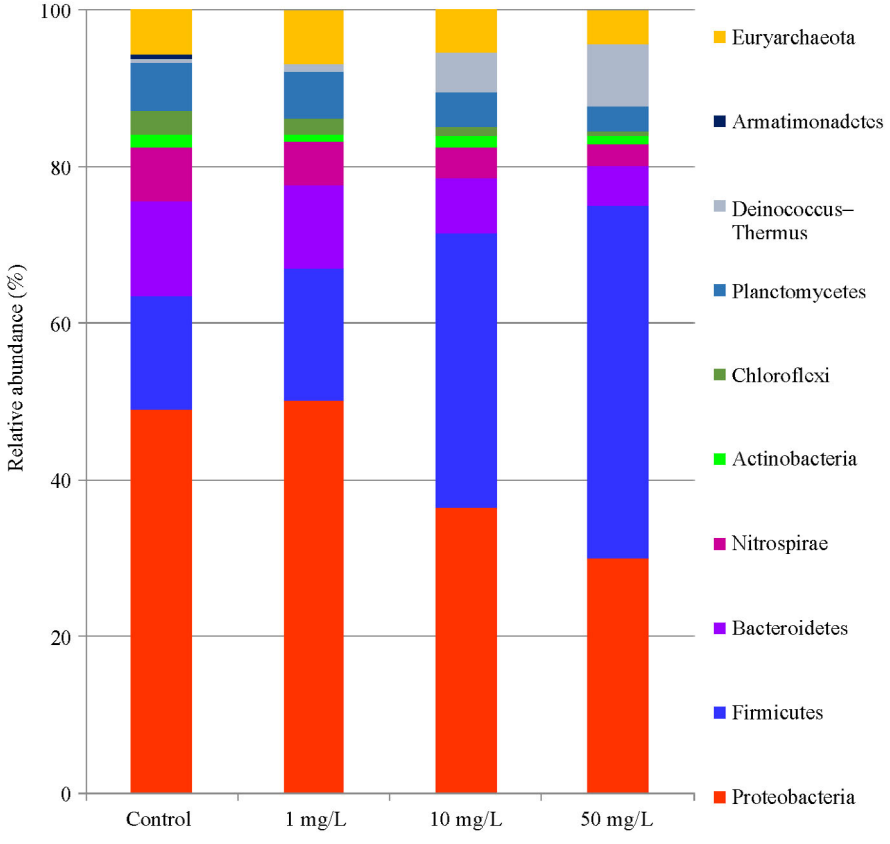

Fig. 6 Relative taxonomic abundance for each sample at the phylum level.

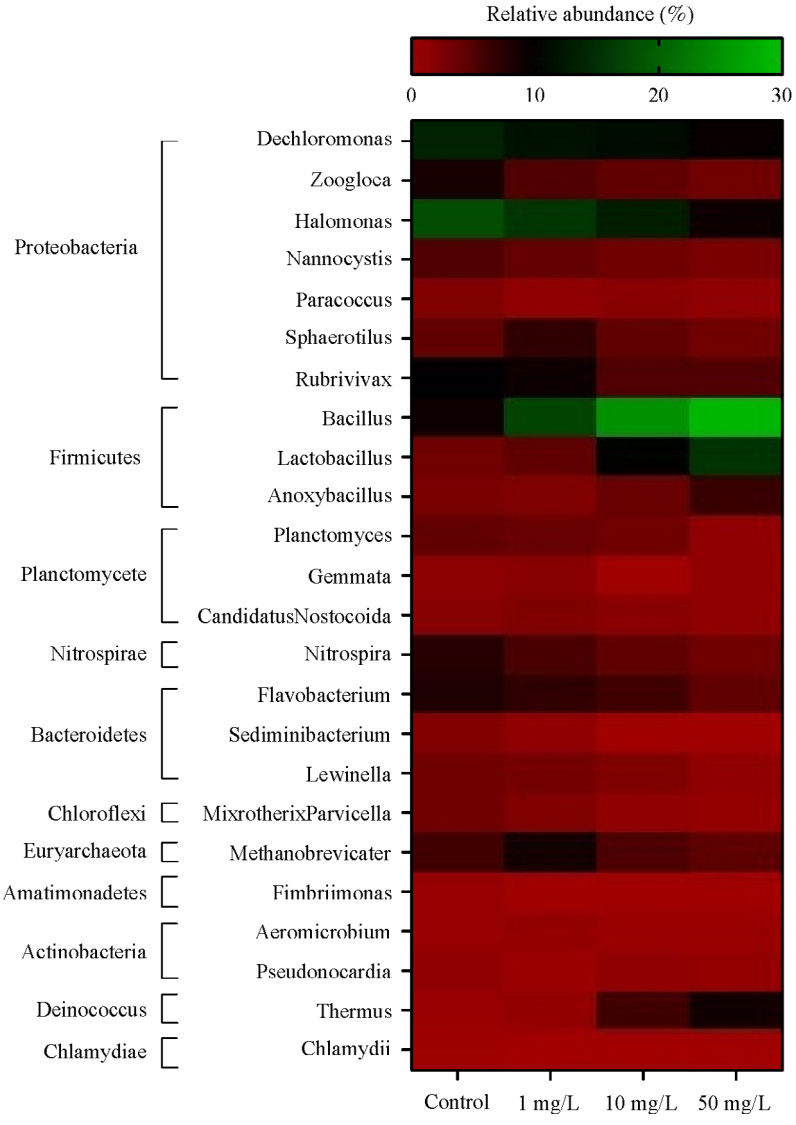

Fig. 7 Heat map analysis of the most abundant genera detected in the GAS in the absence and presence of ZnO-NPs.

of the bacterial genera was used (Fig. 7). From the genera identified in the samples, 24 genera that had higher abundance were selected for heat-map analysis. The most abundant genera identified were *Dechloromonas, Halomonas, Zoogloea, Bacillus, Flavobacterium, Rubrivivax* and *Nitrospira*. According to the heat-map analysis, in the presence of ZnO-NPs the genera such as *Zoogloea*, *Planctomyces*, *Nitrospira* and *Halomonas* were reduced. Also, *Sediminibacterium* and *Fimbriimonas* genera were completely removed from the reactors. In contrast, after exposure to the NPs the relative abundance of *Bacillus*, *Lactobacillus*, *Thermus*, and *Dechloromonas* increased.

4 Conclusions

The exposure of ZnO-NPs caused a reduction in GAS function on the COD, TN and TP removal and this was attributed to bacterial enzymatic activity decreasing. Toxicity of the ZnO-NPs related to release of Zn^{2+} ions; direct interaction of ZnO-NPs/ Zn^{2+} with cell well or DNA, disruption of cell membrane integrity, and ROS generation. According to the results, long-term exposure to high NPs doses lead to the reduction or the disappearance of some bacteria and had an inhibitory effect on the performance of AS, the compositions of EPS and bacterial enzyme activities. The high abundance of filaments on the GAS surface caused their initial resistance to NPs shock and to protect the bacteria present in the inner GAS layers.

Acknowledgements This work was supported by the vice-chancellor for Research and Technology of Kerman University of Medical Sciences (Grant No. 98001185) and the code of research ethics certificate IR.KMU. REC.1399.415. The authors would like to thank the Environmental Health Engineering Research Center, the Kerman University of Medical Sciences, for their scientific supports.

References

Arnaout C L (2012). Assessing the Impacts of Silver Nanoparticles on the Growth, Diversity, and Function of Wastewater Bacteria, Dissertation for the Doctoral Degree. Durham: Duke University

APHA 2005. Standard Methods for the Examination of Water and Wastewater, Washington, DC: American Public Health Association

Corry B (2008). Designing carbon nanotube membranes for efficient water desalination. Journal of Physical Chemistry B, 112(5): 1427–1434

Chen Y, Su Y, Zheng X, Chen H, Yang H (2012). Alumina nanoparticles-induced effects on wastewater nitrogen and phosphorus removal after short-term and long-term exposure. Water Research, 46(14): 4379–4386

Choi O, Clevenger T E, Deng B, Surampalli R L, Ross J L Jr, Hu Z (2009). Role of sulfide and ligand strength in controlling nanosilver toxicity. Water Research, 43(7): 1879–1886

Daraei H, Rafiee M, Yazdanbakhsh A R, Amoozegar M A, Guanglei Q (2019). A comparative study on the toxicity of nanozero valent iron (nZVI) on aerobic granular sludge and flocculent activated sludge: Reactor performance, microbial behavior, and mechanism of toxicity. Process Safety and Environmental Protection, 129: 238–248

Daraei H, Manshouri M, Yazdanbakhhsh A R (2010). Removal of phenol from aqueous solution using ostrich feather ash. Majallah-i Danishgah-i Ulum-i Pizishki-i Mazandaran, 20(79): 81–87

Decker T, Lohmann-Matthes M L (1988). A quick and simple method for the quantitation of lactate dehydrogenase release in measurements of cellular cytotoxicity and tumor necrosis factor (TNF) activity. Journal of Immunological Methods, 115(1): 61–69

Deng S H, Wang L, Su H (2016). Role and influence of extracellular polymeric substances on the preparation of aerobic granular sludge. Journal of Environmental Management, 173: 49–54

Gottschalk F, Sonderer T, Scholz R W, Nowack B (2009). Modeled environmental concentrations of engineered nanomaterials (TiO_2, ZnO, Ag, CNT, fullerenes) for different regions. Environmental Science & Technology, 43(24): 9216–9222

Gonzalez-Estrella J, Sierra-Alvarez R, Field A J (2013). Toxicity assessment of inorganic nanoparticles to acetoclastic and hydrogenotrophic methanogenic activity in anaerobic granular sludge. Journal of Hazardous Materials, 260: 278–285

Jiang H, Mashayekhi W, Xing B (2009). Bacterial toxicity comparison between nano- and micro-scaled oxide particles. Environmental Pollution, 157(5): 1619–1625

Kaegi R, Voegelin A, Sinnet B, Zuleeg S, Hagendorfer H, Burkhardt M, Siegrist H (2011). Behavior of metallic silver nanoparticles in a pilot wastewater treatment plant. Environmental Science & Technology, 45(9): 3902–3908

Kiser M A, Ryu H, Jang H Y, Hristovski K, Westerhoff P (2010). Biosorption of nanoparticles to heterotrophic wastewater biomass. Water Research, 44(14): 4105–4114

Kim B, Park C S, Murayama M, Hochella M F Jr (2010). Discovery and characterization of silver sulphide nanoparticles in final sewage sludge products. Environmental Science & Technology, 44(19): 7509–7514

Labbé N, Parent S, Villemur R (2003). Addition of trace metals increases denitrification rate in closed marine systems. Water Research, 37(4): 914–920

Li Z, Wang X, Ma B, Wang S, Zheng D, She Z, Guo L, Zhao Y, Xu Q, Jin C, Li S, Gao M (2017). Long-term impacts of titanium dioxide nanoparticles (TiO2 NPs) on performance and microbial community of activated sludge. Bioresource Technology, 238: 361–368

Li H, Shen T T, Wang X L, Lin K F, Liu Y D, Lu S G, Gu J D, Wang P, Lu Q, Du X M (2013). Biodegradation of perchloroethylene and chlorophenol co-contamination and toxic effect on activated sludge performance. Bioresource Technology, 137: 286–293

Liang Z H, Das A, Hu Z Q (2010). Bacterial response to a shock load of nanosilver in an activated sludge treatment system. Water Research, 44(18): 5432–5438

Marcilhac C, Sialve B, Pourcher A M, Ziebal C, Bernet N, Beline F (2014). Digestate color and light intensity affect nutrient removal and competition phenomena in a microalgal–bacterial ecosystem. Water Research, 64: 278–287

Mu H, Zheng X, Chen Y, Chen H, Liu K (2012). Response of anaerobic granular sludge to a shock load of zinc oxide nanoparticles during biological wastewater treatment. Environmental Science & Technology, 46(11): 5997–6003

Mu H, Chen Y G (2011). Long-term effect of ZnO nanoparticles on waste activated sludge anaerobic digestion. Water Research, 45(17): 5612–5620

Ni S Q, Ni J, Yang N, Wang J (2013). Effect of magnetic nanoparticles on the performance of activated sludge treatment system. Bioresource Technology, 143: 555–561

Quan X, Cen Y, Lu F, Gu L, Ma J (2015). Response of aerobic granular sludge to the long-term presence to nanosilver in sequencing batch reactors: reactor performance, sludge property, microbial activity and community. Science of the Total Environment, 506-507: 226–233

Sheng G P, Yu H Q, Li X Y (2010). Extracellular polymeric substances (EPS) of microbial aggregates in biological wastewater treatment systems: A review. Biotechnology Advances, 28(6): 882–894

Sirelkhatim A, Mahmud S, Seeni A, Kaus N H M, Ann L C, Bakhori S K M, Hasan H, Mohamad D (2015). Review on zinc oxide nanoparticles: Antibacterial activity and toxicity mechanism. Nano-Micro Letters, 7(3): 219–242

Siddiqi K S, ur Rahman A, Tajuddin, Husen A (2018). Properties of zinc oxide nanoparticles and their activity against microbes. Nanoscale Research Letters, 13(1): 141–148

Tan M, Qiu G, Ting Y.P (2015). Effects of ZnO nanoparticles on wastewater treatment and their removal behavior in a membrane bioreactor. Bioresource Technology, 185: 125–133

Weinberg F, Hamanaka R, Wheaton W W, Weinberg S, Joseph J, Lopez M, Kalyanaraman B, Mutlu G M, Budinger G R S, Chandel N S (2010). Mitochondrial metabolism and ROS generation are essential for mediated tumorigenicity. Proceedings of the National Academy of Sciences of the United States of America, 107(19): 8788–8793

Yazdanbakhsh A R, Rafiee M, Daraei H, Amoozegar M A (2019). Responses of flocculated activated sludge to bimetallic Ag-Fe nanoparticles toxicity: Performance, activity enzymatic, and bacterial community shift. Journal of Hazardous Materials, 366: 114–123

Yamamoto O, Komatsu M, Sawai J, Nakagawa Z E (2004). Effect of lattice constant of zinc oxide on antibacterial characteristics. Journal of Materials Science. Materials in Medicine, 15(8): 847–851

Yang Y, Wang J, Xiu Z, Alvarez P J (2013). Impacts of silver nanoparticles on cellular and transcriptional activity of nitrogen-cycling bacteria. Environmental Toxicology and Chemistry, 32(7): 1488–1494

Zheng X, Wu R, Chen Y (2011). Effects of ZnO nanoparticles on wastewater biological nitrogen and phosphorus removal. Environmental Science & Technology, 45(7): 2826–2832

Zheng Y M, Yu H Q, Liu S H, Liu X Z (2006). Formation and instability of aerobic granules under high organic loading conditions. Chemosphere, 63(10): 1791–1800